

Laboratory Evolution of Robust and Enantioselective Baeyer–Villiger Monooxygenases for Asymmetric Catalysis

Manfred T. Reetz* and Sheng Wu

Max-Planck-Institut für Kohlenforschung, Kaiser-Wilhelm-Platz 1, 45470 Mülheim an der Ruhr, Germany

Received July 24, 2009; E-mail: reetz@mpi-muelheim.mpg.de

Abstract: The Baeyer–Villiger Monooxygenase, Phenylacetone Monooxygenase (PAMO), recently discovered by Fraaije, Janssen, and co-workers, is unusually thermostable, which makes it a promising candidate for catalyzing enantioselective Baeyer–Villiger reactions in organic chemistry. Unfortunately, however, its substrate scope is very limited, reasonable reaction rates being observed essentially only with phenylacetone and similar linear phenyl-substituted analogs. Previous protein engineering attempts to broaden the range of substrate acceptance and to control enantioselectivity have been met with limited success, including rational design and directed evolution based on saturation mutagenesis with formation of focused mutant libraries, which may have to do with complex domain movements. In the present study, a new approach to laboratory evolution is described which has led to mutants showing unusually high activity and enantioselectivity in the oxidative kinetic resolution of a variety of 2-aryl and 2-alkylcyclohexanones which are not accepted by the wild-type (WT) PAMO and of a structurally very different bicyclic ketone. The new strategy exploits bioinformatics data derived from sequence alignment of eight different Baeyer–Villiger Monooxygenases, which in conjunction with the known X-ray structure of PAMO and induced fit docking suggests potential randomization sites, different from all previous approaches to focused library generation. Sites harboring highly conserved proline in a loop of the WT are targeted. The most active and enantioselective mutants retain the high thermostability of the parent WT PAMO. The success of the “proline” hypothesis in the present system calls for further testing in future laboratory evolution studies.

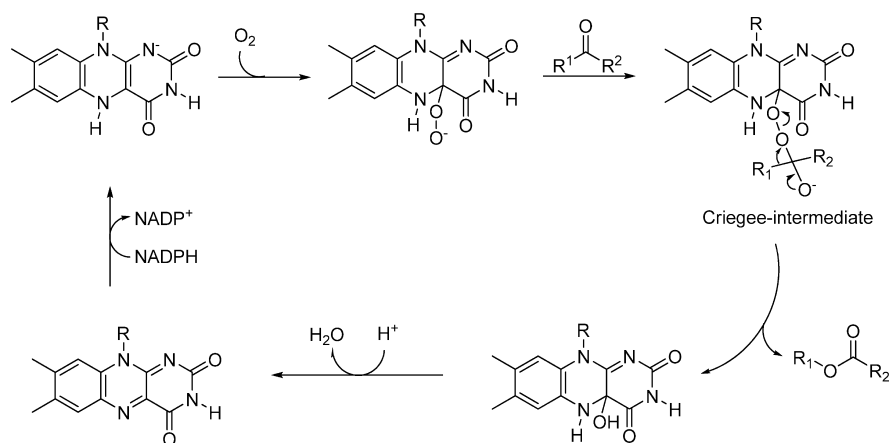
Introduction

Catalytic asymmetric Baeyer–Villiger (BV) reactions of ketones with formation of chiral esters or lactones constitute synthetically attractive transformations in organic chemistry.¹ This type of enantioselective C–C bond activation can be catalyzed by chiral transition metal complexes^{1,2} or organocatalysts^{1–3} using stoichiometric amounts of H₂O₂, per-acids, or alkylhydroperoxides. However, high levels of enantioselectivity and activity are only possible with strained ketones such as cyclobutanone derivatives. Enzymatic processes employing

appropriate monooxygenases, specifically Baeyer–Villiger Monooxygenases (BVMOs) in the presence of oxygen (air) as the oxidant, are an attractive alternative,^{1c,4} as originally shown by Taschner using a cyclohexanone monooxygenase (CHMO).⁵ The catalytic profile of these enzymes in terms of activity, substrate scope, and enantioselectivity is remarkable, yet notable limitations persist to this day.^{1c,4} These monooxygenases are flavin-dependent (Scheme 1),^{4,6} which means that cofactor regeneration of expensive NADPH is necessary when using isolated enzymes.⁷ Fusion proteins comprising BVMOs and phosphite dehydrogenase⁷ⁱ (as an NADPH regeneration enzyme) are likewise known.⁸ Thus far, biocatalytic BV reactions have generally been performed with whole cells, biotechnological processes that have been up-scaled in some cases,⁹ but seldom used in normal organic chemistry laboratories.

- (1) Reviews of Baeyer–Villiger reactions: (a) Krow, G. R. *Org. React. (N. Y.)* **1993**, *43*, 251–798. (b) Renz, M.; Meunier, B. *Eur. J. Org. Chem.* **1999**, 737–750. (c) ten Brink, G.-J.; Arends, I. W. C. E.; Sheldon, R. A. *Chem. Rev.* **2004**, *104*, 4105–4123.
- (2) (a) Bolm, C.; Schlingloff, G.; Weickhardt, K. *Angew. Chem.* **1994**, *106*, 1944–1946. *Angew. Chem., Int. Ed. Engl.* **1994**, *33*, 1848–1849. (b) Gusso, A.; Baccin, C.; Pinna, F.; Strukul, G. *Organometallics* **1994**, *13*, 3442–3451. (c) Uchida, T.; Katsuki, T. *Tetrahedron Lett.* **2001**, *42*, 6911–6914. (d) Ito, K.; Ishii, A.; Kuroda, T.; Katsuki, T. *Synlett* **2003**, 643–646. (e) Strukul, G. *Angew. Chem.* **1998**, *110*, 1256–1267. *Angew. Chem., Int. Ed.* **1998**, *37*, 1198–1209. (f) Frison, J.-C.; Palazzi, C.; Bolm, C. *Tetrahedron* **2006**, *62*, 6700–6706. (g) Colladon, M.; Scarso, A.; Strukul, G. *Synlett* **2006**, 3515–3520.
- (3) (a) Murahashi, S.-I.; Ono, S.; Imada, Y. *Angew. Chem.* **2002**, *114*, 2472–2474. *Angew. Chem., Int. Ed.* **2002**, *41*, 2366–2368. (b) Imada, Y.; Iida, T.; Murahashi, S.-I.; Naota, T. *Angew. Chem.* **2005**, *117*, 1732–1734. *Angew. Chem., Int. Ed.* **2005**, *44*, 1704–1706. (c) Wang, B.; Shen, Y.-M.; Shi, Y. *J. Org. Chem.* **2006**, *71*, 9519–9521. (d) Peris, G.; Miller, S. J. *Org. Lett.* **2008**, *10*, 3049–3052. (e) Malkov, A. V.; Frisocourt, F.; Bell, M.; Swarbrick, M. E.; Kočovský, P. *J. Org. Chem.* **2008**, *73*, 3996–4003. (f) Xu, S.; Wang, Z.; Zhang, X.; Zhang, X.; Ding, K. *Angew. Chem.* **2008**, *120*, 2882–2885. *Angew. Chem., Int. Ed.* **2008**, *47*, 2840–2843.

- (4) Reviews of Baeyer–Villiger Monooxygenases as catalysts in organic chemistry⁶: (a) Kayser, M. M. *Tetrahedron* **2009**, *65*, 947–974. (b) Stewart, J. D. *Curr. Org. Chem.* **1998**, *2*, 195–216. (c) Flitsch, S.; Grogan, G. In *Enzyme Catalysis in Organic Synthesis*; Drauz, K., Waldmann, H., Eds.; Wiley-VCH: Weinheim, 2002; Vol. 2, pp 1202–1245. (d) Alphand, V.; Carrea, G.; Wohlgemuth, R.; Furstoss, R.; Woodley, J. M. *Trends Biotechnol.* **2003**, *21*, 318–323. (e) Brzostowicz, P. C.; Walters, D. M.; Thomas, S. M.; Nagarajan, V.; Rouvière, P. E. *Appl. Environ. Microbiol.* **2003**, *69*, 334–342. (f) Mihovilovic, M. D. *Curr. Org. Chem.* **2006**, *10*, 1265–1287. (g) Wohlgemuth, R. *Eng. Life Sci.* **2006**, *6*, 577–583. (h) Kamerbeek, N. M.; Janssen, D. B.; Van Berkel, W. J. H.; Fraaije, M. W. *Adv. Synth. Catal.* **2003**, *345*, 667–678.
- (5) (a) Taschner, M. J.; Black, D. J. *J. Am. Chem. Soc.* **1988**, *110*, 6892–6893. (b) Taschner, M. J.; Black, D. J.; Chen, Q.-Z. *Tetrahedron: Asymmetry* **1993**, *4*, 1387–1390. (c) Taschner, M. J.; Peddada, L. *J. Chem. Soc., Chem. Commun.* **1992**, 1384–1385.

Scheme 1. Simplified Mechanism of BVMOs^{4,6}

In spite of the past successes,^{1c,4} the instability of BVMOs constitutes a point of concern.¹⁰ When using the isolated enzymes in conjunction with an enzymatic NADPH regeneration system (or isolated fusion proteins) in place of whole cells, this factor needs to be considered. Greater robustness would also be advantageous when employing whole cells, either as such or in immobilized form, because this would impart greater robustness to the system under operating conditions. For these reasons, the discovery by Fraaije, Janssen, et al. of a thermostable BVMO, namely phenylacetone monooxygenase (PAMO), was a major step forward.¹¹ Moreover, the X-ray structure analysis of PAMO (in the absence of NADP⁺), reported in 2004 by Malito, Mattevi, and co-workers,¹² provided for the first time a means to consider the mechanism of BVMOs in greater detail

than in the past.⁴ In particular, it was suggested that Arg337 stabilizes the Criegee intermediate by H-bonding,¹² which helps considerably when unravelling the details of the mechanism. Indeed, we utilized this information in discussing the stereochemical outcome of previous BVMO catalyzed reactions such as those reported for CHMO and mutants thereof generated by directed evolution,¹³ yet a detailed interpretation was not possible. Most recently, Lau, Berghuis, and co-workers reported the X-ray structure of a CHMO from an environmental *Rhodococcus* strain not only bound with FAD but also with NADP⁺,¹⁴ showing an open and a closed form in the absence of a substrate or inhibitor. This is highly revealing, but a precise interpretation of the stereochemical outcome of CHMO catalyzed reactions remains a challenge, which may have to do with the complex domain movements and the “sliding” cofactor.

Unfortunately, the substrate scope of the robust wild-type (WT) PAMO is very narrow, reasonable activity being observed essentially only with phenylacetone or similar linear phenyl-substituted ketones.¹¹ In previous protein engineering studies of PAMO, we utilized rationally designed amino acid deletions¹⁵ and saturation mutagenesis using the Combinatorial Active-Site Saturation Test (CAST)¹⁶ at loop positions 441–444 next to the putative binding pocket (Figure 1), drastically reduced amino acid alphabets being used on the basis of sequence alignment of eight BVMOs.¹⁷ These positions, being part of a longer loop, constitute a “bulge” in PAMO, absent in CHMO, and were therefore considered to be promising sites for protein engineering. However, strategies utilizing deletions or randomization at positions 441–444 expanded the substrate scope only minimally. The basic result was the evolution of mutants that catalyze the oxidative kinetic resolution of 2-phenylcyclohexanone with

- (6) Isolation, characterization and/or mechanistic studies of CHMOs and other BVMOs: (a) Turfitt, G. E. *Biochem. J.* **1948**, *42*, 376–383. (b) Donoghue, N. A.; Norris, D. B.; Trudgill, P. W. *Eur. J. Biochem.* **1976**, *63*, 175–192. (c) Schwab, J. M.; Li, W. B.; Thomas, L. P. *J. Am. Chem. Soc.* **1983**, *105*, 4800–4808. (d) Walsh, C. T.; Chen, Y.-C. *J. Angew. Chem.* **1988**, *100*, 342–352. *Angew. Chem., Int. Ed. Engl.* **1988**, *27*, 333–343. (e) Brzostowicz, P. C.; Walters, D. M.; Thomas, S. M.; Nagarajan, V.; Rouvière, P. E. *Appl. Environ. Microbiol.* **2003**, *69*, 334–342. (f) Sheng, D.; Ballou, D. P.; Massey, V. *Biochemistry* **2001**, *40*, 11156–11167.
- (7) (a) Zhao, H.; van der Donk, W. A. *Curr. Opin. Biotechnol.* **2003**, *14*, 583–589. (b) van der Donk, W. A.; Zhao, H. *Curr. Opin. Biotechnol.* **2003**, *14*, 421–426. (c) de Gonzalo, G.; Ottolina, G.; Carrea, G.; Fraaije, M. W. *Chem. Commun. (Cambridge, U. K.)* **2005**, 3724–3726. (d) Hollmann, F.; Taglieber, A.; Schulz, F.; Reetz, M. T. *Angew. Chem.* **2007**, *119*, 2961–2964. *Angew. Chem., Int. Ed.* **2007**, *46*, 2903–2906. (e) Hollmann, F.; Hofstetter, K.; Schmid, A. *Trends Biotechnol.* **2006**, *24*, 163–171. (f) Urlacher, V. B.; Schmid, R. D. *Curr. Opin. Chem. Biol.* **2006**, *10*, 156–161. (g) Zambianchi, F.; Pasta, P.; Carrea, G.; Colonna, S.; Gaggero, N.; Woodley, J. M. *Biotechnol. Bioeng.* **2002**, *78*, 489–496. (h) Lee, W.-H.; Park, J.-B.; Park, K.; Kim, M.-D.; Seo, J.-H. *Appl. Microbiol. Biotechnol.* **2007**, *76*, 329–338. (i) Woodyer, R.; van der Donk, W. A.; Zhao, H. *Biochemistry* **2003**, *42*, 11604–11614.
- (8) Torres Pazmiño, D. E.; Snajdrova, R.; Baas, B.-J.; Ghobrial, M.; Mihovilovic, M. D.; Fraaije, M. W. *Angew. Chem.* **2009**, *120*, 2307–2310. *Angew. Chem., Int. Ed.* **2008**, *47*, 2275–2278.
- (9) (a) Hilker, I.; Wohlgenuth, R.; Alphand, V.; Furstoss, R. *Biotechnol., Bioeng.* **2005**, *92*, 702–710. (b) Baldwin, C. V. F.; Wohlgenuth, R.; Woodley, J. M. *Org. Process Res. Dev.* **2008**, *12*, 660–665.
- (10) Walton, A. Z.; Stewart, J. D. *Biotechnol. Prog.* **2004**, *20*, 403–411.
- (11) (a) Fraaije, M. W.; Wu, J.; Heuts, D. P. H. M.; van Hellemond, E. W.; Spelberg, J. H. L.; Janssen, D. B. *Appl. Microbiol. Biotechnol.* **2005**, *66*, 393–400. (b) Zambianchi, F.; Fraaije, M. W.; Carrea, G.; de Gonzalo, G.; Rodríguez, C.; Gotor, V.; Ottolina, G. *Adv. Synth. Catal.* **2007**, *349*, 1327–1331. (c) Rodríguez, C.; de Gonzalo, G.; Torres Pazmiño, D. E.; Fraaije, M. W.; Gotor, V. *Tetrahedron: Asymmetry* **2008**, *19*, 197–203.
- (12) Malito, E.; Alfieri, A.; Fraaije, M. W.; Mattevi, A. *Proc. Natl. Acad. Sci. U.S.A.* **2004**, *101*, 13157–13162.

- (13) (a) Reetz, M. T.; Brunner, B.; Schneider, T.; Schulz, F.; Clouthier, C. M.; Kayser, M. M. *Angew. Chem.* **2004**, *116*, 4167–4170. *Angew. Chem., Int. Ed.* **2004**, *43*, 4075–4078. See also directed evolution for increasing the enantioselectivity of the BVMO from *Pseudomonas fluorescens*: (b) Kirschner, A.; Bornscheuer, U. T. *Appl. Microbiol. Biotechnol.* **2008**, *81*, 465–472.
- (14) Mirza, I. A.; Yachnin, B. J.; Wang, S.; Grosse, S.; Bergeron, H.; Imura, A.; Iwaki, H.; Hasegawa, Y.; Lau, P. C. K.; Berghuis, A. M. *J. Am. Chem. Soc.* **2009**, *131*, 8848–8854.
- (15) (a) Boccola, M.; Schulz, F.; Leca, F.; Vogel, A.; Fraaije, M. W.; Reetz, M. T. *Adv. Synth. Catal.* **2005**, *347*, 979–986. (b) Schulz, F.; Leca, F.; Hollmann, F.; Reetz, M. T. *Beilstein J. Org. Chem.* **2005**, *1*, 10.
- (16) (a) Reetz, M. T.; Boccola, M.; Carballeira, J. D.; Zha, D.; Vogel, A. *Angew. Chem.* **2005**, *117*, 4264–4268. *Angew. Chem., Int. Ed.* **2005**, *44*, 4192–4196. (b) Reetz, M. T.; Kahakeaw, D.; Sanchis, J. *Mol. Biosyst.* **2009**, *5*, 115–122.
- (17) Reetz, M. T.; Wu, S. *Chem. Commun. (Cambridge, U. K.)* **2008**, 5499–5501.

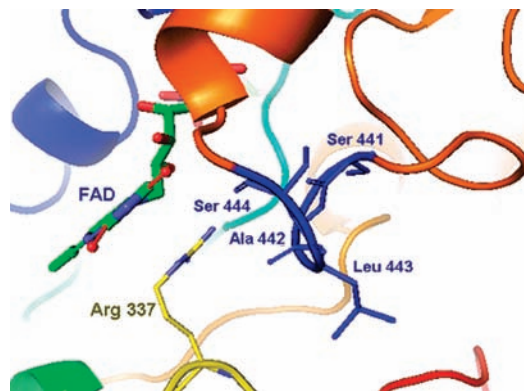


Figure 1. Excerpt of WT PAMO structure based on the X-ray data in the absence of a substrate or inhibitor, featuring the oxidized flavin (FAD), Arg337 presumably stabilizing the Criegee intermediate, and the 441–444 loop segment (“bulge”) directly aligning the putative binding pocket (chosen in previous studies for protein engineering).^{15,17}

reasonable reaction rate and high enantioselectivity ($E = 30\text{--}70$ in favor of the respective *R*-lactone), compared to the WT PAMO which shows a minimal rate and thus low conversion (<10% after extended reaction times) as well as stereorandom behavior ($E \approx 1$).¹⁷ Later work showed that 2-alkyl substituted cyclohexanone derivatives such as 2-methyl- or 2-ethylcyclohexanone are not at all accepted by these mutants nor by WT PAMO.¹⁸ In another study, rationally designed PAMO mutant Met466Gly proved to be a useful catalyst for enantioselective sulfoxidation of some prochiral thio-ethers, but broadening the substrate scope of BV reactions proved to be difficult.^{11b} Thus, the need to perform further research was obvious.

Directed evolution of enzymes has emerged as a powerful method to engineer such catalytic properties as thermostability, robustness toward hostile solvents as well as substrate scope and enantioselectivity, error-prone PCR, DNA shuffling and saturation mutagenesis being the most popular gene mutagenesis techniques.^{19,20} When targeting substrate scope and/or enantioselectivity using saturation mutagenesis, amino acid positions aligning the binding pocket are generally chosen as randomization sites with formation of so-called focused libraries.^{15,16,19–23} Here we describe an unconventional strategy for focused library production which involves randomization at sites quite different from those based on the conventional procedure, specifically by focusing on a residue which appears to be spatially further

away (second sphere residue). Since we succeeded in evolving pronounced activity and high enantioselectivity in BV reactions using very small mutant libraries (and thus minimal experimental effort), while maintaining high thermostability inherent in WT PAMO, our study constitutes a significant step forward in this field of catalytic oxidation. Moreover, due to their high thermostability, it is possible to use the BVMO mutants in isolated form in combination with a secondary alcohol dehydrogenase (2°ADH) as an NADPH regeneration system with isopropanol serving as the stoichiometric reductant, if so desired.

Results and Discussion

Exploratory Experiments Based on the Conventional Approach to Saturation Mutagenesis.

In directed evolution of enantioselective enzymes based on saturation mutagenesis with formation of focused libraries,^{20,21} a strategy first reported in 2001,²² it is necessary to choose randomization sites next to the binding pocket, preferably in a systematic way as in CASTing.^{16,20,21} If the X-ray structure (or homology model) is available, preferably with a bound substrate or inhibitor, the choice is generally straightforward. However, if no structural data of substrate or inhibitor bound enzyme is accessible, the choice may be difficult to make, certainly when studying fluxional enzymes known to undergo substantial internal movements (in the extreme case allosteric motion). BVMOs appear to belong to this category.^{1c,4} As noted above, loop optimization by randomizing those positions in PAMO which appear to align the putative binding pocket of the ligand-free enzyme, positions 441–444 (Figure 1), led only to partial success.¹⁷ In hope of obtaining a more realistic “picture” of the putative binding pocket, we performed induced fit docking experiments of WT PAMO utilizing the X-ray data¹⁰ and phenylacetone as the substrate. The result indicates that the substrate and catalytically important Arg337 are both located on the *re*-side of the flavin (FAD), substantiating expectations (Figure 2). The distance between the oxygen atom of phenylacetone and the C4a atom of FAD is about 6.6 Å, which means that the intermediate deprotonated flavin-hydroperoxide (Scheme 1) appears to be spatially close enough to the carbonyl function of the substrate for smooth BV reaction to occur.

Close inspection of the docking result reveals the presence of 17 amino acids within the range of about 5 Å around the substrate, namely Gln152, Leu153, Ser196, Lys336, Arg337, Ile339, Gly388, Phe389, Asp390, Ala391, Leu392, Ala442, Met446, Ser500, Trp501, Met515 and Leu516 (Figure S1/Supporting Information), which are all potential sites for CASTing. At this stage several strategic decisions appeared logical, e.g., the generation of 17 individual saturation mutagenesis libraries, or libraries resulting from grouping several amino acid positions together. Based on Figure 1 (and Figure S1/Supporting Information) and previous experience regarding loop optimization,¹⁷ we proceeded by choosing five randomization sites (Figure S2/Supporting Information), specifically 441/442/443/444 (site A), 445/446 (B), 152/153 (C), 338/339 (D)

(18) Wu, S.; Reetz, M. T. Unpublished results, 2008.

(19) Reviews of directed evolution: (a) Lutz, S.; Bornscheuer, U. T. *Protein Engineering Handbook*, Vol. 1–2; Wiley-VCH: Weinheim, Germany, 2009. (b) Arndt, K. M.; Müller, K. M. *Protein Engineering Protocols (Methods in Molecular Biology)*, Vol. 352; Humana Press: Totowa, NJ, 2007. (c) Arnold, F. H.; Georgiou, G. *Methods and Molecular Biology*, Vol. 230; Humana Press: Totowa, NJ, 2003. (d) Jäckel, C.; Kast, P.; Hilvert, D. *Annu. Rev. Biophys. Biomol. Struct.* **2008**, *37*, 153–173. (e) Brakmann, S.; Schwienhorst, A. *Evolutionary Methods in Biotechnology - Clever Tricks for Directed Evolution*, Wiley-VCH: Weinheim, Germany, 2004. (f) Hibbert, E. G.; Baganz, F.; Hailes, H. C.; Ward, J. M.; Lye, G. J.; Woodley, J. M.; Dalby, P. A. *Biomol. Eng.* **2005**, *22*, 11–19. (g) Rubin-Pitel, S. B.; Zhao, H. *Comb. Chem. High Throughput Screening* **2006**, *9*, 247–257. (h) Kaur, J.; Sharma, R. *Crit. Rev. Biotechnol.* **2006**, *26*, 165–199. (i) Bershtein, S.; Tawfik, D. S. *Curr. Opin. Chem. Biol.* **2008**, *12*, 151–158. (j) Reetz, M. T. In *Asymmetric Organic Synthesis with Enzymes*; Gotor, V., Alfonso, I., García-Urdiales, E., Eds.; Wiley-VCH: Weinheim, Germany, 2008; pp 21–63.

(20) Reviews of directed evolution of enantioselective enzymes:^{19j} (a) Reetz, M. T. *Proc. Natl. Acad. Sci. U.S.A.* **2004**, *101*, 5716–5722. (b) Reetz, M. T. In *Protein Engineering Handbook*; Lutz, S., Bornscheuer, U. T., Eds.; Wiley-VCH: Weinheim, Germany, 2009; Vol. 2.

(21) (a) Reetz, M. T.; Carballeira, J. D. *Nat. Protoc.* **2007**, *2*, 891–903. See also discussion regarding close and remote mutations:^{19j} (b) Park, S.; Morley, K. L.; Horsman, G. P.; Holmquist, M.; Hult, K.; Kazlauskas, R. *J. Chem. Biol.* **2005**, *12*, 45–54. (c) Horsman, G. P.; Liu, A. M. F.; Henke, E.; Bornscheuer, U. T.; Kazlauskas, R. *J. Chem.—Eur. J.* **2003**, *9*, 1933–1939.

(22) Reetz, M. T.; Wilensek, S.; Zha, D.; Jäger, K.-E. *Angew. Chem.* **2001**, *113*, 3701–3703. *Angew. Chem., Int. Ed.* **2001**, *40*, 3589–3591.

(23) Reetz, M. T.; Kahakeaw, D.; Lohmer, R. *ChemBioChem* **2008**, *9*, 1797–1804.

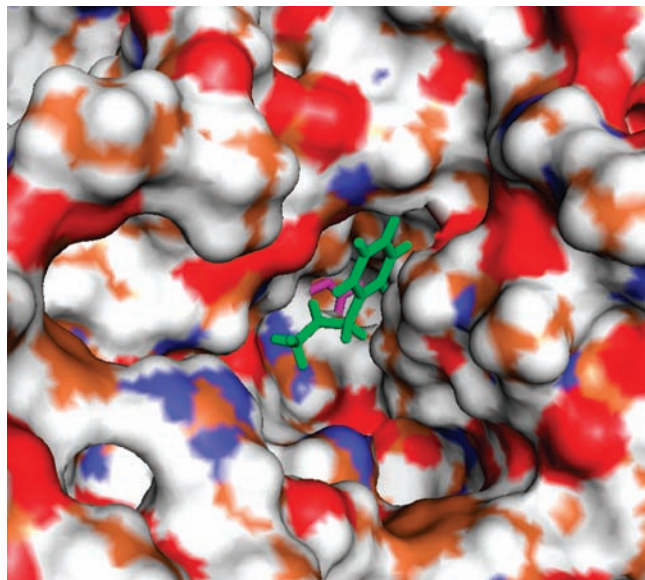


Figure 2. Induced fit docking of phenylacetone in the X-ray structure of WT PAMO¹⁰ featuring this substrate (green sticks) in the putative binding pocket and FAD (magenta sticks).

and 334/335 (E). In order to reduce the screening effort, which is the bottleneck in any directed evolution study,^{19,20} we chose for the different positions reduced amino acid alphabets^{17,23} by applying the respective codon degeneracy (Table S1/Supporting Information). The degree of oversampling corresponding to 95% coverage, calculated by the computer aid CASTER^{21a,24} (based on known algorithms assuming the absence of amino acid bias)²⁵ was found to be within a reasonable range which can be handled by the screening system used in the present study.

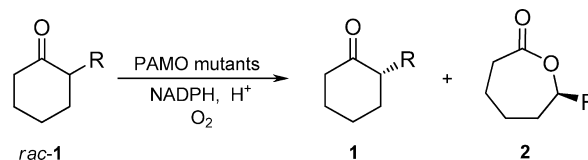
We envisioned the laboratory evolution of PAMO mutants which would not just accept 2-phenylcyclohexanone (**1a**) in a fast reaction, but essentially any 2-substituted cyclohexanone derivative, for example, ketones **1b–1l**, which would broaden the substrate scope of robust PAMO enzymes considerably. As the model reaction for mutagenesis/screening, the BV transformation of ketone **1a** was chosen. We reasoned that if mutants displaying substantial activity were to be found in any of the libraries, then they could be tested for the other more challenging ketones as well. The hope was that active and stereoselective mutants can be identified in this way without performing additional mutagenesis/screening experiments.

Unfortunately, no hits were found in libraries B, C, D, or E, while library A contained, not unexpectedly, several improved mutants that were already known to us from our original (441–444)-loop optimization, which however do not accept 2-alkylcyclohexanone derivatives.^{17,18} Currently, it is difficult to explain these negative results. Rather than continuing the search for sensitive CAST sites or using larger amino acid alphabets for saturation mutagenesis (which could well be successful), we turned to a different strategy.

(24) The CASTER computer aid for designing saturation mutagenesis libraries is available free of charge from the authors homepage: http://www.mpi-muelheim.mpg.de/mpikofo_home.html.

(25) (a) Rui, L.; Kwon, Y. M.; Fishman, A.; Reardon, K. F.; Wood, T. K. *Appl. Environ. Microbiol.* **2004**, *70*, 3246–3252. (b) Bosley, A. D.; Ostermeier, M. *Biomol. Eng.* **2005**, *22*, 57–61. (c) Mena, M. A.; Daugherty, P. S. *Protein Eng., Des. Sel.* **2005**, *18*, 559–561. (d) Denault, M.; Pelletier, J. N. *In Protein Engineering Protocols*; Vol. 352; Arndt, K. M., Müller, K. M., Eds; Humana Press: Totowa, NJ, 2007; pp 127–154.

Scheme 2. Oxidative Kinetic Resolution of *rac*-1 Catalyzed by PAMO Mutants^a



- | | | | |
|---|----------------------|---|--|
| a | R = Phenyl | g | R = <i>n</i> -Butyl |
| b | R = 4-Chlorophenyl | h | R = Allyl |
| c | R = 4-Methylphenyl | i | R = <i>i</i> -Propyl |
| d | R = Methyl | j | R = Cyclohexyl |
| e | R = Ethyl | k | R = Benzyl |
| f | R = <i>n</i> -Propyl | l | R = CH ₂ CH ₂ CN |

^a Note that the *R/S*-designation may change in accord with the CIP priority of the R-substituent of the ketone and lactone.

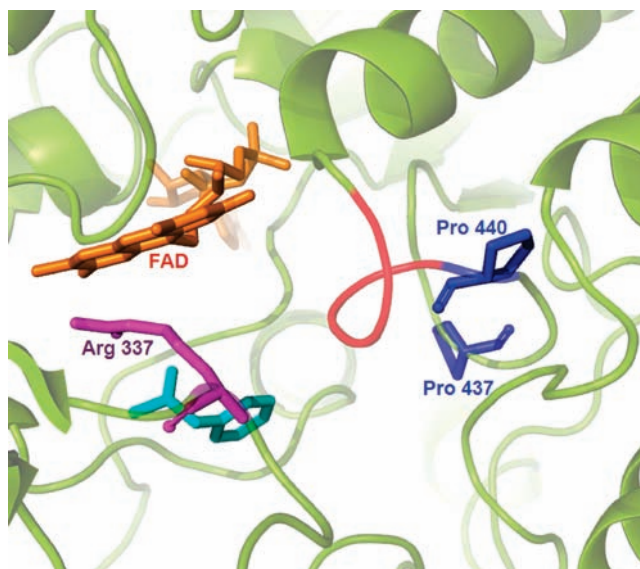


Figure 3. Illustration of the putative binding pocket of PAMO based on the induced fit docking model. Phenylacetone and the loop segment 441–444 are shown in cyan and red, respectively, whereas Pro437 and Pro440 are pictured in blue.

Bioinformatics Approach to Saturation Mutagenesis. In our previous study¹⁷ regarding partial loop optimization at positions 441–444, which according to the ligand-free X-ray structure in combination with the induced fit docking model all have direct contact with the binding pocket (Figure 3), sequence alignment of WT PAMO and seven other BVMOs was used as a guide for choosing reduced amino alphabets in saturation mutagenesis experiments (Figure 4). In contrast to this approach, in the present study we focus on position 440, which according to Figure 3 seems to be a “second sphere” residue,^{19a} that is, the first residue not in apparent direct contact with the binding pocket. Due to the dynamics of PAMO, which may be expected from this enzyme, and the lack of structural data of the ligand-bound form, we realized that this is an uncertain issue. For this very reason we were curious to test position 440, since situations of this kind may arise in diverse future studies of other enzymes as well. It also struck us that proline is highly conserved at this position in BVMOs (Figure 4), an amino acid that is known to impart a certain degree of rigidity in proteins.²⁶ Increasing flexibility by substituting proline for another amino acid could

(26) Fersht, A. *Structure and Mechanism in Protein Science*; W. H. Freeman and Co.: New York, 2000.

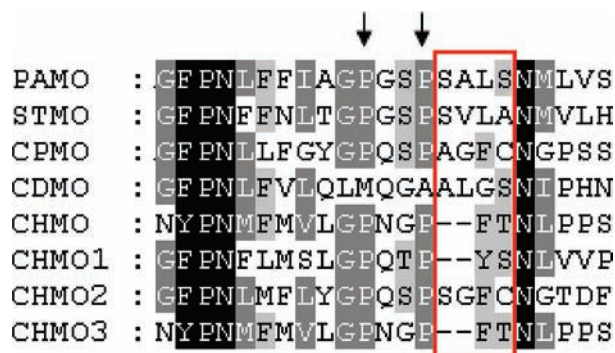


Figure 4. Alignment of eight BVMO protein sequences highlighting loop segment 441–444 (red box) and positions 437 and 440 (arrows) indicating the new sites for saturation mutagenesis. Code: Phenylacetone monooxygenase (PAMO) from *Thermobifida fusca* (1w4x), steroid monooxygenase (STMO) from *Rhodococcus rhodochrous* (BAA24454), cyclohexanone monooxygenase (CHMO) from *Acinetobacter* sp. NCIMB 9871 (BAA86293), cyclohexanone monooxygenase 1 (CHMO1) from *Brevibacterium* sp. HCU (AAG01289), cyclohexanone monooxygenase 2 (CHMO2) from *Brevibacterium* sp. HCU (AAG01290), cyclohexanone monooxygenase 3 (CHMO3) from *Acinetobacter* sp. (P12015), cyclopentanone monooxygenase (CPMO) from *Comamonas testosteroni* (CAD10798), and cyclododecanone monooxygenase (CDMO) from *Rhodococcus ruber* (AAL14233).

well have an impact on the spatial position of the neighboring residues and perhaps of the entire loop by inducing some kind of rearrangement. Along this line of reasoning, a second nearby position also harboring proline, namely Pro437, was likewise considered for saturation mutagenesis.

Two focused libraries were produced by saturation mutagenesis at positions 437 and 440, respectively, using NNK degeneracy encoding all 20 proteinogenic amino acids (QuikChange/Stratagene).²⁷ This time we considered for screening purposes a particularly “difficult” substrate, *rac*-2-ethylcyclohexanone (*rac*-1e), as the model compound in oxidative kinetic resolution. As already mentioned, this compound is not at all transformed by WT PAMO, even after an extended reaction duration of several days.¹⁸ Each library was screened by evaluating about 200 transformants. This was achieved by an activity test, followed by enzyme isolation and kinetic resolution of *rac*-1e in conjunction with the known robust 2°ADH from *Thermoanaerobacter ethanolicus* as the NADPH regeneration enzyme²⁸ using isopropanol as the reductant. Assuming the absence of amino acid bias, this degree of oversampling should be more than sufficient for at least 95% coverage.^{21a,24}

Whereas the focused library corresponding to position 437 failed to contain any active clones, saturation mutagenesis at position 440 resulted in the identification of a number of active and enantioselective mutants. Ten hits were identified and sequenced, five of them showing particularly high activity (the other five were no longer considered for further study, namely Pro440Cys, Pro440Thr, Pro440Lys, Pro440Arg, and Pro440Gly). The selectivity factors *E* of the five active mutants as well as the results of kinetic studies are summarized in Table 1 (entries 1–5). It can be seen that unusually high enzyme activity and enantioselectivity were achieved by this simple and rapid experiment.

We and others have previously pointed out that conventional saturation mutagenesis²⁷ of the type used here and in most other

Table 1. Kinetic Resolution of *rac*-1e using PAMO Mutants Derived from a Saturation Mutagenesis Library (Entries 1–5) or Site-Specific Mutagenesis (Entries 6–7) Both at Position 440

entry	mutant	<i>E</i> -value	<i>K_m</i> (mM)	<i>k_{cat}</i> (s ⁻¹)	<i>k_{cat}/K_m</i> (M ⁻¹ s ⁻¹)
1	Pro440Phe	26	0.89	1.2	1300
2	Pro440Leu	>200	1.6	0.72	450
3	Pro440Ile	>200	2.7	0.66	240
4	Pro440Asn	>200	2.2	1.5	680
5	Pro440His	34	1.0	0.83	830
6	Pro440Trp	>200	1.3	1.3	1000
7	Pro440Tyr	95	1.9	1.1	580

Table 2. *E*-values in the oxidative kinetic resolution of substrates *rac*-1a–1d and *rac*-1f–1l^a

entry	mutant	<i>rac</i> -1a	<i>rac</i> -1b	<i>rac</i> -1c	<i>rac</i> -1d	<i>rac</i> -1f	<i>rac</i> -1g
1	Pro440Leu	42	63	–	>200	>200	>200
2	Pro440Ile	25	ND	–	>200	>200	>200
3	Pro440Asn	18	18	–	>200	>200	>200
4	Pro440His	12	11	–	>200	>200	33
5	Pro440Tyr	11	ND	4	ND	ND	ND
6	Pro440Trp	3.4	ND	30	ND	ND	ND

entry	mutant	<i>rac</i> -1h	<i>rac</i> -1i	<i>rac</i> -1j	<i>rac</i> -1k	<i>rac</i> -1l
7	Pro440Leu	>200	–	>200	–	>200
8	Pro440Ile	34	–	69	–	20
9	Pro440Asn	>200	–	22	–	49
10	Pro440His	37	>200	84	9	146
11	Pro440Tyr	ND	>200	119	ND	>200
12	Pro440Trp	ND	>200	45	19	40

^a ND: not determined, –: low conversion.

studies,^{19–21} although very simple to apply, occurs with some degree of amino acid bias. This may mean that some of the expected amino acid substitutions leading to potential hits are not observed in the screening process even though oversampling has been performed.^{15b,21a,23} In directed evolution studies using saturation mutagenesis this is tolerable, since improved mutants are generally found.¹⁹ Nevertheless, we wanted to check this, which in the present system is an easy endeavor because it involves a single amino acid position. All of the “missing” mutants were prepared by conventional site-specific mutagenesis and tested in the model reaction. Of the nine relevant cases, namely Pro440Ala, Pro440Val, Pro440Ser, Pro440Asp, Pro440Glu, Pro440Gln, Pro440Tyr, Pro440Trp and Pro440Met, two new mutants proved to be active, namely Pro440Tyr and Pro440Trp (Table 1, entries 6–7). Thus, in the present system conventional saturation mutagenesis coupled with theoretically sufficient oversampling assuming the absence of amino acid bias results in 80% hit-identification. This is the first time that such information has been generated, which may be of interest in future directed evolution studies based on saturation mutagenesis. Interestingly, it can be seen that very different types of amino acids replacing Pro440 lead to active and enantioselective catalysts, which means that the factors contributing to catalyst improvement, on a molecular level, must be quite different.

Although no (bio)catalyst can ever be “universal”, organic chemists seek to develop catalysts which function well for a range of different substrates. Therefore, without performing any more mutagenesis experiments, we were keen to test the best mutants, engineered for a single substrate *rac*-1e, as catalysts in the kinetic resolution of a variety of structurally different racemic ketones: *rac*-1a–1d, *rac*-1f–1l and the bicyclic substrate *rac*-3. In these experiments, isolated enzyme mutants were again employed in conjunction with the in vitro use of 2°ADH for NADPH regeneration. As in the case of the model

(27) Hogrefe, H. H.; Cline, J.; Youngblood, G. L.; Allen, R. M. *Biotechniques* **2002**, *33*, 1158–1165.

(28) (a) Zheng, C.; Pham, V. T.; Phillips, R. S. *Bioorg. Med. Chem. Lett.* **1992**, *2*, 619–622. (b) Burdette, D. S.; Tchernajenko, V.; Zeikus, J. G. *Enzyme Microb. Technol.* **2000**, *27*, 11–18.

Table 3. Kinetic Studies of Mutant Pro440Phe as a Catalyst in the Kinetic Resolution of Substrates *rac-1a–1l*

entry	substrate	<i>E</i> -value	<i>K</i> _m (mM)	<i>k</i> _{cat} (s ⁻¹)	<i>k</i> _{cat} / <i>K</i> _m (M ⁻¹ s ⁻¹)
1	<i>rac-1a</i>	12	0.81	1.3	1600
2	<i>rac-1b</i>	7	0.26	0.77	3000
3	<i>rac-1c</i>	117	0.13	0.19	1500
4	<i>rac-1d</i>	95	3.1	1.6	520
5	<i>rac-1e</i>	26	0.89	1.2	1300
6	<i>rac-1f</i>	145	0.70	1.7	2400
7	<i>rac-1g</i>	39	0.34	1.1	3200
8	<i>rac-1h</i>	102	1.1	1.7	1500
9	<i>rac-1i</i>	>200	0.73	0.26	360
10	<i>rac-1j</i>	145	0.26	0.41	1600
11	<i>rac-1k</i>	48	0.16	0.33	2100
12	<i>rac-1l</i>	91	3.8	1.5	390

compound *rac-1e*, the other substrates are likewise not accepted by WT PAMO, with the exception of the 2-phenyl derivatives *rac-1a–1b* which show minimal conversion under extended reaction times but poor enantioselectivity (*E* = 1–2). Gratifyingly, many of the mutants are indeed excellent catalysts in the oxidative kinetic resolution of all of the tested 2-substituted cyclohexanone derivatives (Table 2). In the majority of cases the standard reaction conditions ensure the desired conversion of about 50% within 10 h. Table S5 in the Supporting Information shows the ee-values of all substrates and products at defined conversion.

Variant Pro440Phe, found to be most active for *rac-1e*, was then used as a catalyst in further oxidative kinetic resolutions involving all substrates. The results summarized in Table 3 point to some remarkable effects. Mutant Pro440Phe shows very high activity for almost all substrates. In the case of 2-alkyl substrates (Table 3, entries 4–7), the catalytic efficiency *k*_{cat}/*K*_m correlates well with the chain length. The longer the side-chain, the higher the catalytic efficiency. We explain this by noting that the affinity (*K*_m) increases as the length of the alkyl chain increases, while the activity (*k*_{cat}) remains in the same range. This is an interesting phenomenon, especially when viewing the respective enantioselectivity, which shows an irregular pattern. It is particularly striking and of synthetic significance that even compounds having fairly bulky substituents such as cyclohexyl or benzyl react rapidly (Table 3, entries 10 and 11). In the case of 2-phenylcyclohexanone (*rac-1a*), a notably high value of *k*_{cat}/*K*_m is observed for mutant Pro440Phe, a result that needs to be compared to the published results of a kinetic study using WT PAMO as the catalyst in the kinetic resolution of the same substrate (*k*_{cat} = 0.06 s⁻¹; *K*_m = 5; *k*_{cat}/*K*_m = 10).⁹ This means a rate acceleration by a factor of 1.6 × 10². In the case of the majority of substrates not at all accepted by WT PAMO, it was not possible to quantify the rate acceleration, but it must be substantially higher.

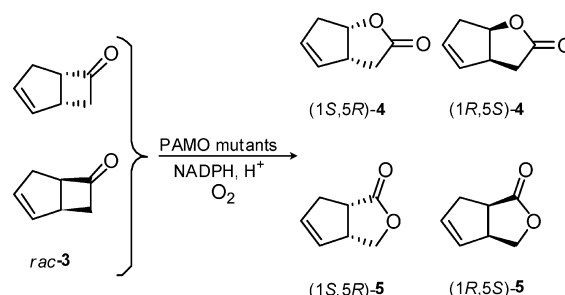
In further work, we tested some of the mutants in the regio- and stereoselective kinetic resolution of a structurally very different substrate, namely *rac-3* with formation of the two regioisomers **4** and **5**, the so-called “normal” and “abnormal” lactones, respectively.⁴ Previous studies regarding the use of other BVMOs in whole cells have in some cases provided high enantioselectivities (>95% ee) and varying degrees of regioselectivity.⁴ The WT PAMO shows a relatively low rate with this substrate, the “normal” lactone **4** being preferred at moderate enantioselectivity.¹⁵ Here again it was of interest to test some of the mutants evolved for substrate *rac-1e* without resorting to any new mutagenesis experiments (Table 4). Importantly, enzyme activity has increased in all cases. It is interesting to

Table 4. Regio- and Enantioselectivity of PAMO Mutants As Catalysts in the BV Reaction of *rac-3*

mutant	conv. (%) ^a	“normal” lactone 4		“abnormal” lactone 5		ratio(4/5)
		ee (%)	abs. conf.	ee (%)	abs. conf.	
WT PAMO	31	86	(1 <i>S</i> ,5 <i>R</i>)	63	(1 <i>S</i> ,5 <i>R</i>)	72:28
Pro440Leu	85	92	(1 <i>S</i> ,5 <i>R</i>)	99	(1 <i>R</i> ,5 <i>S</i>)	52:48
Pro440Ile	89	92	(1 <i>S</i> ,5 <i>R</i>)	93	(1 <i>R</i> ,5 <i>S</i>)	49:51
Pro440Phe	99	94	(1 <i>S</i> ,5 <i>R</i>)	98	(1 <i>R</i> ,5 <i>S</i>)	48:52
Pro440Tyr	89	92	(1 <i>S</i> ,5 <i>R</i>)	97	(1 <i>R</i> ,5 <i>S</i>)	46:54
Pro440Trp	86	87	(1 <i>S</i> ,5 <i>R</i>)	97	(1 <i>R</i> ,5 <i>S</i>)	48:52
Pro440Asn	85	92	(1 <i>S</i> ,5 <i>R</i>)	97	(1 <i>R</i> ,5 <i>S</i>)	49:51
Pro440His	82	92	(1 <i>S</i> ,5 <i>R</i>)	95	(1 <i>R</i> ,5 <i>S</i>)	47:53

^a Reaction time: 10 h.

note that WT PAMO favors the formation of **4** as the (1*S*,5*R*)-enantiomer and also produces some of **5** as the (1*S*,5*R*)-enantiomer, whereas the mutants lead to a reversal of enantioselectivity in the case of regioisomer **5** (Table 4).



Thermostability of Evolved PAMO Mutants. While performing the above experiments, we noticed qualitatively that the mutants appear to retain high thermostability characteristic of WT PAMO. In order to check quantitatively whether the thermostability of the PAMO variants has suffered to any notable degree as a consequence of mutagenesis, the *T*₅₀⁶⁰ values were measured for the best mutants. This is the temperature at which a heat treatment for one hour reduces enzyme activity by 50%.²⁹ The measured *T*₅₀⁶⁰ value of WT PAMO (58.2 °C) and those of the best mutants Pro440Phe (56.2 °C), Pro440Tyr (56.7 °C), Pro440Trp (56.3 °C), Pro440His (55.8 °C), Pro440Leu (56.0 °C), Pro440Ile (56.0 °C) and Pro440Asn (56.3 °C) show that the mutational changes do not impair the unique high thermostability of the enzyme to any significant degree (Figure 5). This was also checked by monitoring the residual activity as a function of time, the BV-reaction of phenylacetone serving as the transformation. No loss of activity was observed when the mutant enzymes were kept at 50 °C for 40 h (data not shown). Again, it can be seen that thermostability is not significantly impaired by the mutational changes.

Conclusions

We have devised a new strategy in directed evolution in order to construct a robust experimental platform for asymmetric Baeyer–Villiger reactions based on the thermostable monooxygenase PAMO. Since WT PAMO accepts only phenylacetone and structurally similar linear phenyl-substituted ketones with reasonable rates, the goal was to expand the substrate scope, i.e., to increase the reaction rate significantly, and to reach high

(29) Reviews of enzyme thermostabilization by protein engineering: (a) Eijsink, V. G. H.; Gåseidnes, S.; Borçhert, T. V.; van den Burg, B. *Biomol. Eng.* **2005**, *22*, 21–30. (b) Ó’Fágáin, C. *Enzyme Microb. Technol.* **2003**, *33*, 137–149. (c) Bommarius, A. S.; Broering, J. M. *Biocatal. Biotransform.* **2005**, *23*, 125–139.

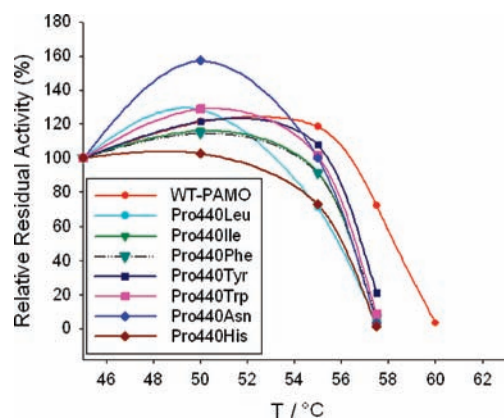


Figure 5. Thermostability of WT-PAMO and its mutants as measured by the relative residual activity as a function of temperature, the BV-transformation of phenylacetone serving as the model reaction.

enantioselectivity, without compromising thermostability. This was indeed achieved. Mutants were evolved which show unusually high activity and enantioselectivity in the oxidative kinetic resolution of a variety of structurally different 2-substituted aryl- and alkylcyclohexanone derivatives and of a structurally unrelated bicyclic ketone. High thermostability is a notable advantage when using BVMOs in whole-cell setups, but also when choosing to apply them in isolated enzyme form. Although the former is generally preferred in industrial applications,⁴ we have demonstrated that the latter in vitro process poses no problems, a secondary alcohol dehydrogenase in combination with the reductant isopropanol serving as the NADPH regeneration system.^{15b} Thus, the present study constitutes a further step to more economically and ecologically viable BVMO-mediated stereoselective Baeyer–Villiger reactions in organic chemistry.⁹

Just as importantly, a new strategy in laboratory evolution was proposed and implemented experimentally. It goes beyond the traditional generation of focused libraries at sites aligning the binding pocket,^{16,17,19–23} and may therefore be useful in other future directed evolution studies. Whenever a given enzyme under study is likely to undergo notable conformational changes due to inherent flexibility, including domain movements, and only its ligand-free X-ray structure is known, then the traditional approach based on saturation mutagenesis at sites seemingly aligning the binding pocket may prove to be problematic. This was the case in the present study. Therefore, a bioinformatics approach to defining randomization sites likely to be hot spots was devised in which the first step involves sequence alignment of eight BVMOs. Guided by the identification of high homology sites and the results of induced fit docking of phenylacetone in the ligand-free X-ray structure, we proceeded to focus on what appeared to be second sphere residues (although they may not actually be so!). Since in any enzyme the number of second sphere residues is much higher than those directly next to the binding pocket,²¹ systematic saturation mutagenesis as in CASTing¹⁶ at all of them would entail a labor-intensive screening effort. In order to circumvent this, an appropriate choice regarding a select number of such randomization sites (hot spots) had to be made. The present study shows that the focus on proline sites in a loop can be rewarding.³⁰ This choice was made in the expectation that the introduction of a more “flexible” amino acid in place of proline can change

the shape, positioning and dynamics of a loop and therefore the environment at the nearby binding pocket and/ influence complex domain movements. However, presently we do not for certain that such a mutation does in fact increase flexibility.

The actual laboratory evolution was performed with a single substrate, *rac*-2-ethylcyclohexanone (**1e**), by applying saturation mutagenesis at two sites, which required the screening of only 200 transformants in each case. The mini-library at one of the single residue sites resulted in half a dozen hits showing high activity and enantioselectivity. Screening a total of only 400 transformants in the present project is an extremely small number in laboratory evolution, the usual libraries employing other techniques generally comprising 10^3 – 10^6 mutants.¹⁹ These biocatalysts, differing by only one point mutation with respect to the WT PAMO, were subsequently tested with 12 other structurally different ketones without performing any further mutagenesis/screening experiments, which led to the discovery that the mutants not only retain their thermostability, but also have a respectably broad substrate acceptance and excellent stereoselectivity. Generalizing the “proline” hypothesis,³⁰ especially in loops of enzymes that undergo (unidentified) internal motions, as well as identifying the reasons for enhanced activity and enantioselectivity in the system described herein are the subjects of future studies.

Experimental Section

Induced Fit Molecular Docking. Commercial software was used in all cases.³¹ The ligand phenylacetone was treated using the program LigPrep of Maestro 8.0 (Schrödinger LLC). OPLS_2005 force field was used to optimize the geometry and minimize the energy. Wide type PAMO crystal structure (PDB code: 1w4x) was optimized by the Protein Preparation Wizard. The missing hydrogen atoms were added, bond orders and formal charges were adjusted, and all the water molecules were removed. After hydrogen bonds were optimized, the obtained structure was further subjected to minimize the energy using the default 0.3 Å rmsd tolerance.

The induced fit docking studies were performed using the Induced Fit Docking protocol of Maestro 8.0. The center of the Glide enclosing box was the centroid of residues Arg 337, Gln 152, Leu 153, Ala442 and Trp 501 based on the catalytic mechanism of PAMO. In the first step of Glide ligand docking, Arg 337 was chosen to temporarily remove the side chains and replaced with Ala. The Coulomb-vdW scaling factors were changed to the default values of 0.7 and 0.5 for the protein and ligand, respectively. A maximum of 20 poses were retained. In the second phase of docking, the Prime application reversed the temporary replacement of Arg 337 with Ala, refined nearby residues, and optimized side chains. In the final docking phase, the ligand was redocked into all induced fit protein structures that were within 30 kcal/mol of the lowest energy structure using the Glide SP scoring function. A maximum of 20 poses were needed. Each was ranked using the composite induced fit score. Each pose was further analyzed manually to determine the substrate binding mode, the distance between the flavin C4a atom and the oxygen atom of the ligand. The best induced fit docking parameters were as follows: docking score = -5.05 kcal/mol, IDFScore = -1355.9 kcal/mol, prime energy = -27018.2 kcal/mol. The distance between the oxygen atom of phenylacetone and C4a atom of FAD was 6.64 Å.

Mutant Library Preparation. The plasmid pPAMO contains the WT PAMO gene (*pamo*) under the control of the P_{BAD} promoter.^{11a} The libraries A, B, C, D, E, F, G and H at the corresponding sites were created by the QuikChange PCR method²⁷ with the template pPAMO and the primers (Table S2/Supporting

(30) Conversely, proline scanning throughout a loop may likewise constitute a useful strategy.

(31) Schrödinger Suite 2007 Induced Fit Docking protocol; Glide version 4.5, Schrödinger LLC, New York, NY, 2005; Primer version 1.6, LLC, New York, NY, 2005.

Information). The reaction (50 μL final volume) contained: 10 \times KOD buffer (5 μL), MgCl_2 (2 μL , 25 mM), dNTP (5 μL , 2 mM each), primers (5 μL , 2.5 μM each), template plasmid (2 μL , 10 ng μL^{-1}) and 1 unit of KOD DNA polymerase. The PCR cycle consisted of an initial denaturation step at 94 $^\circ\text{C}$ for 3 min followed by cycling at 94 $^\circ\text{C}$ for 1 min and 72 $^\circ\text{C}$ for 14 min for 20 cycles, then a final elongation for 35 min at 72 $^\circ\text{C}$. The template plasmid in 26 μL PCR amplification reaction was removed by digestion with 1 unit of Dpn I (New England Biolabs) in 3 μL of NEB buffer 4 for 2–3 h at 37 $^\circ\text{C}$. The resulting PCR product was used to transform into electrocompetent *Escherichia coli* TOP10 cells. The cells were spread on LB agar plates containing 100 $\mu\text{g mL}^{-1}$ carbenicilline. For the primers used in site-specific mutagenesis, see Table S3/Supporting Information.

Library Screening. Individual colonies were placed into 2.2-mL 96-deep-well plates containing 800 μL of LB media with 100 $\mu\text{g mL}^{-1}$ carbenicilline by a colony picker QPIX (Genetix, New Milton, UK). After cell growth at 37 $^\circ\text{C}$ overnight with shaking at 800 rpm, 10 μL of each preculture was transferred into a new plate containing 800 μL of TB media supplemented with 0.1% L-arabinose as inducer and 100 $\mu\text{g mL}^{-1}$ carbenicilline. The duplicate plates were grown for additional 24 h to induce PAMO expression. The cultures were centrifuged at 4000 rpm and 4 $^\circ\text{C}$ for 6 min and the supernatants were discarded. The original plates were stored. Each cell pellet was resuspended in 600 μL of 50 mM Tris-HCl (pH 8.0) containing 1 mg mL^{-1} lysozyme and 4 units of Dnase I. Lysis were performed at 37 $^\circ\text{C}$ and 800 rpm for 3 h. Cell debris was precipitated by centrifugation at 4000 rpm and 4 $^\circ\text{C}$ for 30 min and 50 μL of each cleared supernatant transferred to a 1.1-mL 96-deep-well plate. Then in each well, 50 μL of the secondary alcohol dehydrogenase (2 $^\circ$ ADH) crude extract (about 10 U),^{15b} 10 μL of 1 mM NADP^+ , 10 μL of 100 mM *rac-1a* (or *rac-1e*) in acetonitrile and 380 μL of 50 mM Tris-HCl (pH 8.0) containing 5 mM isopropanol were added. The reaction plates were incubated at 37 $^\circ\text{C}$ and 800 rpm for 24 h. Four-hundred microliters of ethyl acetate was then added to each well, and a plastic cover was used to cover the plate tightly. The plate was vibrated vigorously to extract the substrate and product from the solution. After centrifugation, 200 μL of organic layer in each well was transferred into a new glass-made 96-deep-well plate, and subjected to GC analysis for screening. Active clones were collected and the results reproduced. The entire gene of the identified hits was sequenced to confirm there were not any other mutations.

Enzyme Expression and Purification. The plasmid pPAMO (WT and the corresponding mutants) was transformed into *Escherichia coli* TOP 10 cells and grown at 37 $^\circ\text{C}$ in LB media with 100 $\mu\text{g mL}^{-1}$ carbenicilline. Two mL of overnight cultures of WT PAMO and mutants in LB media containing 100 $\mu\text{g mL}^{-1}$ carbenicilline were transferred into 200 mL TB media with 0.1% L-arabinose as inducer and 100 $\mu\text{g mL}^{-1}$ carbenicilline, and incubated at 37 $^\circ\text{C}$ with shaking at 250 rpm for 24 h. Cells were harvested by centrifugation and washed once with 0.9% NaCl solution. The cell pellets were resuspended in 10 mL 50 mM Tris-HCl buffer (pH 8.0) and lysed by sonification. The cell debris was removed by centrifugation at 10 000 rpm for 30 min at 4 $^\circ\text{C}$. The supernatant was filtered and loaded on a GE Healthcare HisTrap FF Crude column (5 mL) pre-equilibrated with 50 mM Tris-HCl buffer containing 0.5 M NaCl and 5 mM imidazol. Impurity was removed by imidazol at the concentration of about 25 mM and the enzyme was eluted by 50 mM Tris-HCl buffer with 0.5 M NaCl and 200 mM imidazol. The enzyme fraction was desalted and concentrated by ultrafiltration using Millipore's Amicon Ultra-15 centrifugal filter devices and then dissolved in 50 mM Tris-HCl buffer (pH 8.0) and stored at -80°C . The purity of the enzyme was measured by SDS-PAGE (Figure S3/Supporting Information). The concentration of the purified enzyme was determined by measuring the absorbance at 441 nm using an extinction coefficient of 12.4 $\text{mM}^{-1}\text{cm}^{-1}$.

Procedure for the Enzymatic Oxidation of Substrates. In a typical protocol, 1 mL reaction system consists of 2.5 mM substrate, 5 mM isopropanol, 100 μM NADP^+ , 0.1–0.5 μM purified PAMO mutant enzyme, secondary alcohol dehydrogenase (2 U), 2.5% acetonitrile and 50 mM Tris-HCl buffer (pH 8.0). For *rac-1b*, 1 equivalent of additional β -cyclodextrin was also added to increase the solubility. The mixture in 8 mL glass tube with a sealed cap (to avoid evaporation of 2-alkyl substituted substrates) was shaken at 200 rpm and 30 $^\circ\text{C}$ for times established to control the conversion rate less than 50% for kinetic resolution. The reaction was stopped, worked up by extraction with ethyl acetate (containing 200 mg L^{-1} internal standard as nonane, dodecane, hexadecane and octadecane). The sample was analyzed by achiral and chiral GC in order to determine the conversion of and the enantiomeric excess of the residual ketones and produced lactones. Control experiments were performed for all the tested substrates with purified WT PAMO enzymes (about 5 μM). It should be noted that a minimal amount (<3%) of 2-methylcyclohexanol was produced in the case of substrate *rac-1d*. For all the other substrates, no reduction products were observed. As for oxidation of *rac-3*, the parallel experiments were performed with the same concentration of enzymes (WT-PAMO and mutants, 0.3 μM) and *rac-3* (2.5 mM). The other components in the reaction system were the same as above (without β -cyclodextrin) and the reaction time was 10 h.

Starting Substrates (Ketones) and Products (Lactones). Ketones *rac-1g*, *1i*, and *1j* were prepared by alkylation as described.^{32a} Ketone *rac-1b* and *1c* were prepared by the reported method,^{32b} and the others purchased from Sigma-Aldrich, Acros, TGI, and Fluka (used without further purification). The racemic lactones were prepared by conventional BV-oxidation of the corresponding ketones using *m*-chloroperoxybenzoic acid (mCPBA). All of the synthesized compounds were isolated by silica gel chromatography and identified by ^1H and ^{13}C NMR.

Identification of Products from Biotransformation. After extraction as described above, the ketones and lactones were identified by comparison of their retention times on GC (HP-5 and the corresponding chiral separation columns) with authentic racemic compounds.

Determination of the Enantiomeric Excess of Residual Ketones and Produced Lactones. The ee values of residual ketones **1** and lactones **2** were determined by chiral GC directly except for ketone **1b** and lactone **2b**, whose ee values were determined separately. Table S4 (Supporting Information) lists the details regarding the chiral separation conditions for each compound tested. The absolute configurations were made by comparison with authentic samples and referring to the literature,^{4b} the respective lactones being prepared by using the recombinant CHMO from *Acinetobacter* sp. NCIMB 9871 as a catalyst in the reaction of ketones **1d–1i** and **1l**, and P3-PAMO mutant for preparing **2a** and **2k**.^{33,15a} The (tentative) assignment of the absolute configuration of lactone **2b–2c** and **2j** was made on the basis of analogy. All *E*-values were calculated using the equation of Sih.³⁴

Steady-State Kinetics. The activities of the purified enzymes were determined spectrophotometrically by monitoring the decrease in the level of NADPH over time at 25 $^\circ\text{C}$ and 340 nm ($\epsilon_{340} = 6.22\text{ mM}^{-1}\text{cm}^{-1}$). The reaction mixture (1.0 mL) contained 50 mM Tris-HCl (pH 8.0), 100 μM NADPH, 0.2–4 mM substrate, 2% acetonitrile, 0.1–0.6 μM purified enzyme. The kinetics measurements were performed on a Molecular Devices Spectramax

(32) (a) Malosh, C. F.; Ready, J. M. *J. Am. Chem. Soc.* **2004**, *126*, 10240–10241. (b) Xie, J.-H.; Liu, S.; Huo, X.-H.; Cheng, X.; Duan, H.-F.; Fan, B.-M.; Wang, L.-X.; Zhou, Q.-L. *J. Org. Chem.* **2005**, *70*, 2967–2973.

(33) (a) Stewart, J. D.; Reed, K. W.; Martinez, C. A.; Zhu, J.; Chen, G.; Kayser, M. M. *J. Am. Chem. Soc.* **1998**, *120*, 3541–3548. (b) Berezina, N.; Kozma, E.; Furstoss, R.; Alphan, V. *Adv. Synth. Catal.* **2007**, *349*, 2049–2053.

(34) Chen, C. S.; Fujimoto, Y.; Grirdaukas, G.; Shi, C. J. *J. Am. Chem. Soc.* **1982**, *104*, 7294–7299.

(Molecular Devices GmbH, Germany). The obtained data were fitted to the Michaelis–Menten equation by nonlinear regression analysis. For measuring the thermostability of the WT PAMO and mutants, solutions of the purified enzymes (about 30 μM) were incubated at 50, 55, 57, and 60 $^{\circ}\text{C}$ for 1 h. The residual activity was determined as described above in the presence of 2 mM phenylacetone. The thermostability of the mutant enzymes was also measured as a function of time at 50 $^{\circ}\text{C}$, the residual activity being determined as above.

Acknowledgment. Financial aid by the Fonds der Chemischen Industrie is gratefully acknowledged. We also thank Petra Wedemann for synthesizing some of the compounds, Jutta Rosentreter for the carefully performed chiral GC analyses, and Dr. Despina Bougiokou for helpful discussions.

Supporting Information Available: Induced fit docking model (Figure S1), picture of sites 437 and 440 in PAMO at which saturation mutagenesis was applied (Figure S2), choice of codon degeneracies (Table S1), primers used in generating libraries A–G (Table S2), primers used in saturation mutagenesis at position 440 (Table S3), purification of PAMO and mutants (Figure S3), chiral GC separation conditions (Table S4) and ee-values of substrates **1a–1** and products **2a–1** in kinetic resolution at defined conversions (Table S5). This material is available free of charge via the Internet at <http://pubs.acs.org>.

JA906212K